AIP | Journal of Applied Physics

The effect of Bi composition on the properties of InP1xBix grown by liquid phase epitaxy

T. D. Das

Citation: Journal of Applied Physics **115**, 173107 (2014); doi: 10.1063/1.4873640
View online: http://dx.doi.org/10.1063/1.4873640
View Table of Contents: http://scitation.aip.org/content/aip/journal/jap/115/17?ver=pdfcov
Published by the AIP Publishing

The effect of Bi composition on the properties of $InP_{1-x}Bi_x$ grown by liquid phase epitaxy

T. D. Das[a)]
Department of Electronic Science, University of Calcutta, 92, A. P. C. Road, Kolkata 700009, India

(Received 9 October 2013; accepted 16 April 2014; published online 6 May 2014)

$InP_{1-x}Bi_x$ epilayers ($x \geq 1.2\%$) on InP (001) are grown reproducibly by liquid phase epitaxy with conventional solution baking in a H_2 environment. The Bi composition and surface morphology of the grown layers are studied by secondary ion mass spectroscopy and atomic force microscopy, respectively. High-resolution x-ray diffraction is used to characterize the lattice parameters and the crystalline quality of the layers. 10 K photoluminescence measurements indicate three clearly resolved peaks in undoped InP layers with band-to-band transition at 1.42 eV which is redshifted with Bi incorporation in the layer with a maximum band gap reduction of 50 meV/% Bi. The effect is attributed to the interaction between the valence band edge and Bi-related defect states as is explained here by valence-band anticrossing model. Room temperature Hall measurements indicate that the mobility of the layer is not significantly affected for Bi concentration up to 1.2%.
 [http://dx.doi.org/10.1063/1.4873640]

I. INTRODUCTION

The alloying of III-V semiconductor with small amount of Bi produces an anomalously large reduction of band gap by as much as 84–90 meV/% Bi (Refs. 1–4) and a huge shift of the split-off band offering further opportunities for the design of spintronic devices,[5] reduce the content of non-III-V species, e.g., Si, in the lattice and leads to the reduction of the point defect and dislocation density in the material. An isoelectronic impurity is generated by substituting a host atom with an impurity that has the same valence electron structure as the host atom to change material quality. The Bi atoms are incorporated into GaP or InP as isovalent impurities due to their electronegativity and ionization energy being significantly lower than those of P. The impurities lead to a dispersionless Bi band below the valence band edge which couples to the valence bands of GaP or InP yielding mixed states. Bi indeed forms pseudodonor bound states in GaP which lies only 100 meV above the valence band maximum.[6] In the III-P compounds, very few investigations have been reported regarding isoelectronic traps related to Bi in GaP[6] and in InP.[7]

The valence band anticrossing (VBAC) model was developed to explain the unusual features of the electronic structure of isoelectronic impurities with larger atomic radius than the host atom in III-V compound semiconductor, such as $GaSb_xAs_{1-x}$ and $GaBi_xAs_{1-x}$ (Ref. 8) and the results show the explicit restructuring of the valence band, and an upward movement of the heavy hole (HH)and light-hole (LH) E_+ bands leading to a reduction of the band gap.

We have earlier reported a liquid phase epitaxy (LPE) technique for the growth of GaSbBi (Ref. 9) and InSbBi.[10,11] Here, we have used the same technique for the growth of InPBi layers and studied their properties, the details of which are being presented in this paper. Further, we have used a VBAC model to explain the bowing behaviour of the valence bands.

II. EXPERIMENT

The samples were grown in a horizontal sliding boat LPE reactor made using a semi-transparent gold furnace (*Thermcraft, Inc., USA*) inside which a high purity quartz reactor tube (*Heraeus Quarzglas, Germany*) was inserted. Layers were grown on (100) oriented Fe-doped semi-insulating InP substrates. Initially, 99.99999% pure In (*Arnaud SAS., France*) along with 1, 1.5, 2, and 3 wt. % (0.55, 0.83, 1.1, and 1.65 at. % Bi in melt) of 99.9999% pure Bi granules (*Azelis France*) were loaded into the boat made up of high density graphite and baked at 800 °C for 20 h under Pd-diffused hydrogen flow to reduce any oxides and other volatile impurities in the metals. The molten metal was next placed over a cleaned and etched undoped polycrystalline InP wafer (*JMC, Ltd., USA*) and baked for 1 h at 650 °C to completely saturate the metal with phosphorous. After the saturation procedure, the melt was moved away from the InP wafer and baked further at 700 °C for 5 h for impurity removal. Final liquidus temperature of the melt was found to be around 647–655 °C. Growth was typically done for 5–8 min under a melt super cooling of 6–7 °C and a constant cooling rate of 0.3 °C/min. Growth was carried out on ⟨100⟩ Fe-doped semi-insulating InP substrates for 8–10 min under a constant cooling rate of 0.2 °C/min after super cooling the melt by 5–6 °C. We have also grown some InP layers without any Bi in the melt for comparison.

Nomarski differential interference contrast microscopy and Atomic force microscopy (AFM) were used to characterize the surface morphology and the thickness of the epilayers. The total epilayer thickness was between 3 and 4 μm. All the samples were studied by high-resolution x-ray diffraction (HRXRD) after the epitaxial growth to determine their crystalline quality and strain status. X-ray coupled $\omega/2\theta$ measurements of (004) plane reflection were preformed systematically with copper target ($\lambda_{CuK\alpha1} = 1.54056$ Å) radiation from a Standard 2.2 kW sealed tube X-ray generator using *Jordon valley's* D1 Evaluation X-ray diffraction

[a)]Electronic mail: tddas@hotmail.com

instrument. The incorporation of Bi in the solid and its depth profile was confirmed by secondary ion mass spectroscopy (SIMS) using a *Hiden* SIMS work station. O_2^+ ion beam of energy 5 keV and 400 nA ions were used to sputter the samples during depth profile measurements. The base pressure in the measurement chamber was 1×10^{-9} millibars or lower and for closing measurement it was about 8×10^{-8} millibars. Since solubility of Bi is 0.55 at. % in Indium. InPBi is a newly attracted material, the SIMS measurement parameters were first calibrated using a InBi thin film grown by LPE with known composition and was estimated to be less than $\sim 2 \times 10^{19}$ cm^{-3}. The samples also contained some unintentional impurities. Low temperature photoluminescence (PL) measurements were done on the samples in an *APD Cryogenics* closed cycle helium cryostat. PL excitation was provided by 532 nm chopped light from a diode pumped solid state laser (*RGBLase LLC, USA*). Luminescence from the layer surface was analyzed using a 0.5 m spectrometer (*Acton Research Corporation, USA*) with a resolution of ~0.2 nm and detection was done in a cooled InGaAs detector coupled with a *Stanford* lock-in amplifier. An intermediate intensity of excitation 1 W/cm^2 was used.

Room temperature Hall effect measurements were done on the samples using van der Pauw technique under a magnetic field of 4 kG. Ohmic contacts were made using annealed 90%In + 10%Sn at the four corners of square-shaped (4×4 mm^2) samples.

III. RESULTS AND DISCUSSION

Figure 1(a) shows the typical SIMS depth profile for the sample IPB3B. The three key elements In(115 and 226), P(31), and Bi(209) are examined. The Bi concentration is maximum at the surface which slowly reduces along the thickness of the layer due to the growth done from a varying-volume solution-melt. A clear interface between the epitaxial InPBi layer and the InP substrate is observed at a depth of about 3.1 μm as shown in Fig. 1(b). The profile of the Bi distribution is determined by the feed velocity of an additional solution-melt.[12]

(004)HRXRD measurement is done on four InPBi samples grown with successively increasing Bi in the melt. Fig. 2 shows typical XRD scans obtained for two of the layers. The peak at ω-$2\theta = 0$ corresponds to the InP substrate and a second peak which is being attributed to InPBi is clearly resolved at higher angle. However, a lattice contraction is observed from measured diffraction pattern instead of a lattice dilation which is as expected after Bi addition. This might be due to the cubic (InP)-to-tetragonal (InBi) phase transformation as Bi is incorporated into InP. The XRD results of our samples grown with different Bi compositions have a smaller full-width-at-half-maximum (FWHM) value compared to molecular beam epitaxy (MBE) and MOVPE grown III-V-bismides,[2,13–15] corresponding to superior crystallinity obtained by LPE growth. The FWHM of different peaks are 0.01°, 0.021°, 0.03°, and 0.05°, respectively. From the angular separation of the two peaks, we are able to calculate the decrease in lattice constant and increase in strain due to Bi incorporation in accordance with Vegard's law using

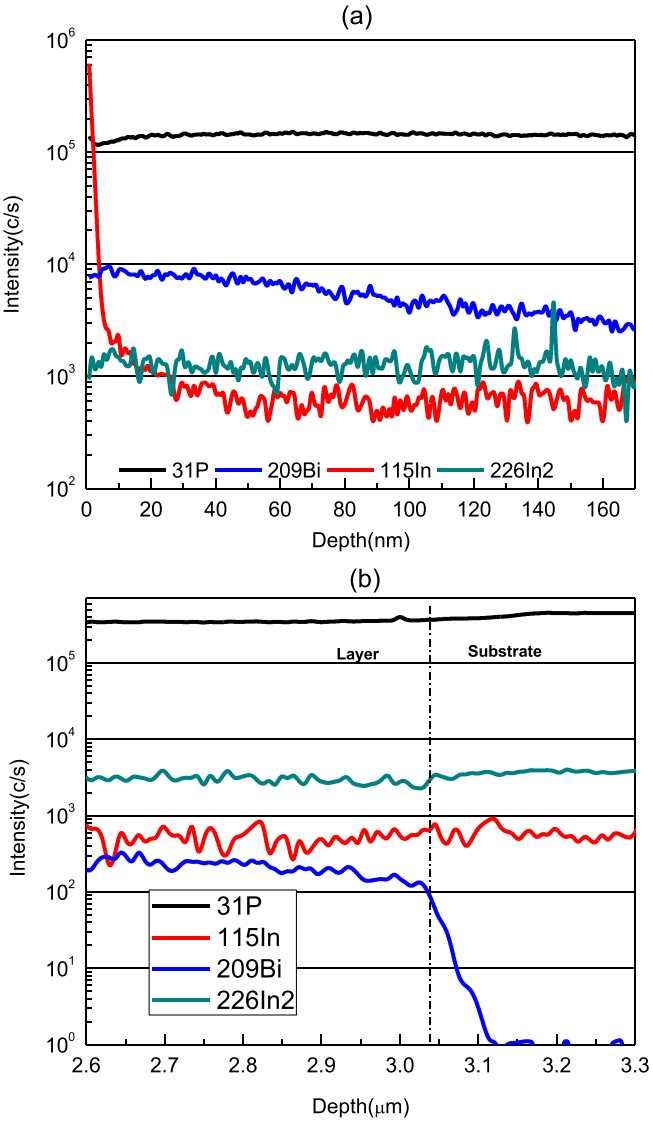

FIG. 1. SIMS profile of different elements in InPBi grown at 637 °C.

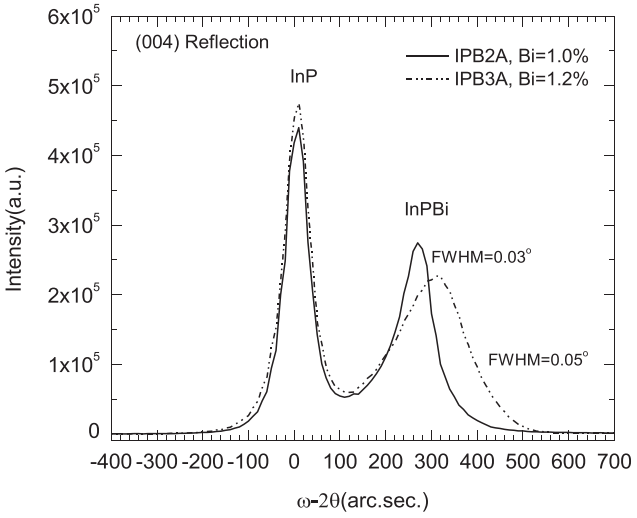

FIG. 2. High resolution X-ray diffraction $\omega/2\theta$ pattern from (004) lattice plane of InPBi/InP epitaxial layers for two samples grown at different temperatures.

lattice constant of 7.024 Å for zinc-blende InBi extrapolated from XRD results.[16]

Normalized Bi intensity from SIMS measurements, which can be an indicator for Bi concentration, is calculated and shown in Fig. 3. It can be found out that the increase in Bi concentration follows the increased Bi composition in the epitaxial layer measured by SIMS up to a Bi content of 1.2%. Bi concentrations measured by SIMS in the four samples are 0.5%, 0.8%, 1.0%, and 1.2%. Since the lattice constant of layers measured by XRD corresponds that incorporated at the substitutional sites only, the result suggests that for higher amount of Bi in the growth melt, a part of the Bi atoms go to the interstitial sites in the InPBi lattice. The trend of lattice contraction follows the normalized Bi concentration deduced from SIMS. Comparing with the lattice constant of InP of 5.8683 Å, a lattice contraction of 0.0145 is found for the sample IPB3A which corresponds to a net lattice mismatch of 0.24% for the layer with the substrate. The lattice contraction is due to Bi segregation and higher Bi concentration leads to strong lattice contraction as suggested earlier.[17]

In Fig. 4, the roughness of the layer surface is plotted against the Bi composition for the samples investigated. InPBi samples (IPB1A, IPB2A, and IPB3A) containing 0.5%, 1.0%, and 1.2% Bi were grown at the growth temperature of 652, 642, and 637 °C, respectively. Decrease in growth temperature is due to the fact that addition of Bi lowered the liquidus temperature of the melt. For lower Bi content of 0.5% in the solid, the surface has an rms roughness of 82 nm. However, an increase in Bi content resulted in extended atomically flat terraces accompanied by a decrease in the rms roughness down to approximately 42 nm for the sample with Bi content of 1.2%. We believe that the observed smoothening of the layer surface is due to a surfactant effect of Bi as was earlier observed in GaAsBi layers grown by molecular beam epitaxy.[18]

The low temperature PL (10 K) spectra of one InP and three InPBi layers with 0.5%, 1.0%, and 1.2% Bi are shown in Fig. 5. The undoped InP sample (Fig. 5(a)) shows three well defined transitions at ~1.42 eV, ~1.38 eV, and 1.34 eV

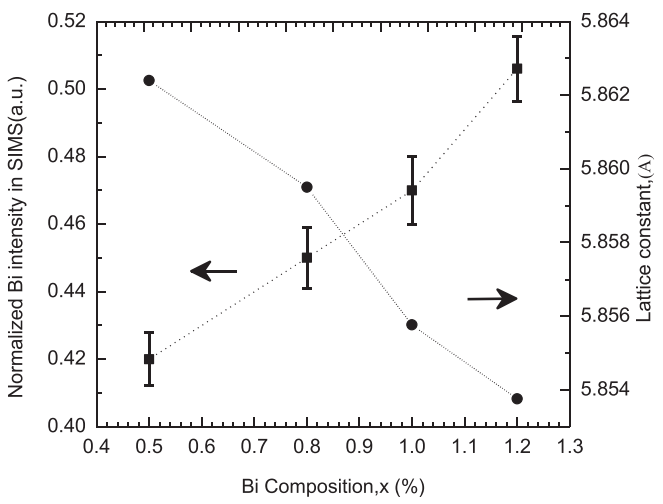

FIG. 3. Normalized Bi concentration obtained from SIMS and the lattice constant deduction from the HRXRD data for $InP_{1-x}Bi_x$.

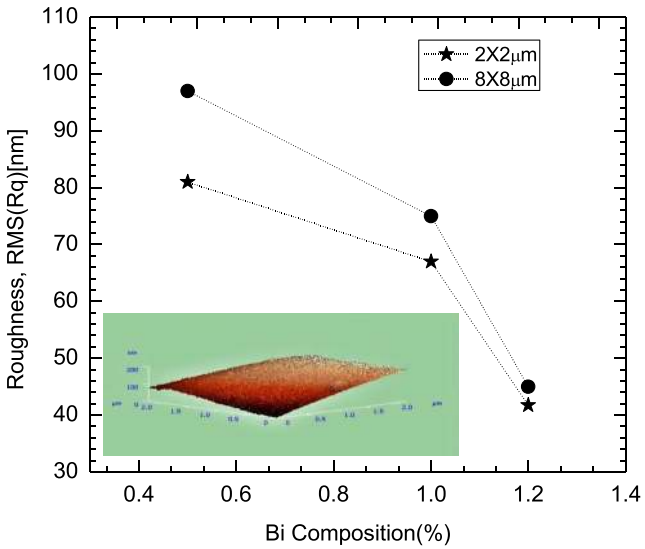

FIG. 4. Roughness obtained from AFM studies as a function of Bi composition. RMS roughness in units of nm obtained from $2 \times 2\,\mu m^2$ to $8 \times 8\,\mu m^2$ scans is shown before and after the slash, respectively.

corresponding to band-to-band (BB),[19] donor-acceptor (DA) pair,[20] and complex defect[21,22] recombinations, respectively. All three Bi containing samples have the BB transition slightly red-shifted by 7 nm with very low intensity and this transition from InP substrate due to excitation laser penetrated the thin grown layer. As expected the PL peak energy decreases with increasing Bi content. The peak energy from band edge transition are 1.38, 1.37, and 1.36 eV for the layers with 0.5%, 1.0%, and 1.2% Bi, respectively. The band gap reduction by ~50 meV/% Bi is significant when compared to the band gap variation of other alloys like GaAsBi,[2] GaSbBi,[9,23,24] etc. In the $InP_{1-x}Bi_x$ layers with $x = 0.005$, 0.010, and 0.012, the prominent donor-acceptor pair transitions are found to be at 1.33, 1.32, and 1.31 eV, respectively.

In support of VBAC calculations, we have considered Type I band alignment between InP and InBi. The calculated bandgap of InBi is found out to be −1.62 eV.[25] In this case, the BAC interaction is expected to occur in the valence band including the HH, LH, and spin-orbit split-off bands. Therefore, as per our calculation, the interaction of the Bi impurity state with the valence band of InP can be best described by the 4×4 matrix Hamiltonian which is given as

$$\begin{pmatrix} H & 0 & V(x) & 0 \\ 0 & L & 0 & V(x) \\ V(x) & 0 & E_{imp} & 0 \\ 0 & V(x) & 0 & E_{imp-SO} \end{pmatrix},$$

where the terms, $H = L = \Delta E_{VBM}x$ and $S = \Delta E_{SO}x$, here ΔE_{VBM} and ΔE_{SO} are the total differences in valence-band maximum and spin-orbit band energies at the Γ point where $k = 0$, E_{imp} is the energy of the Bi-related resonant defect state, V(x) is the composition-dependent interaction matrix element. The valence band offset (VBO) between the end-point compounds in $InP_{1-x}Bi_x$ is found out to be 1.30 eV by extrapolating the graph of valence band offsets and the

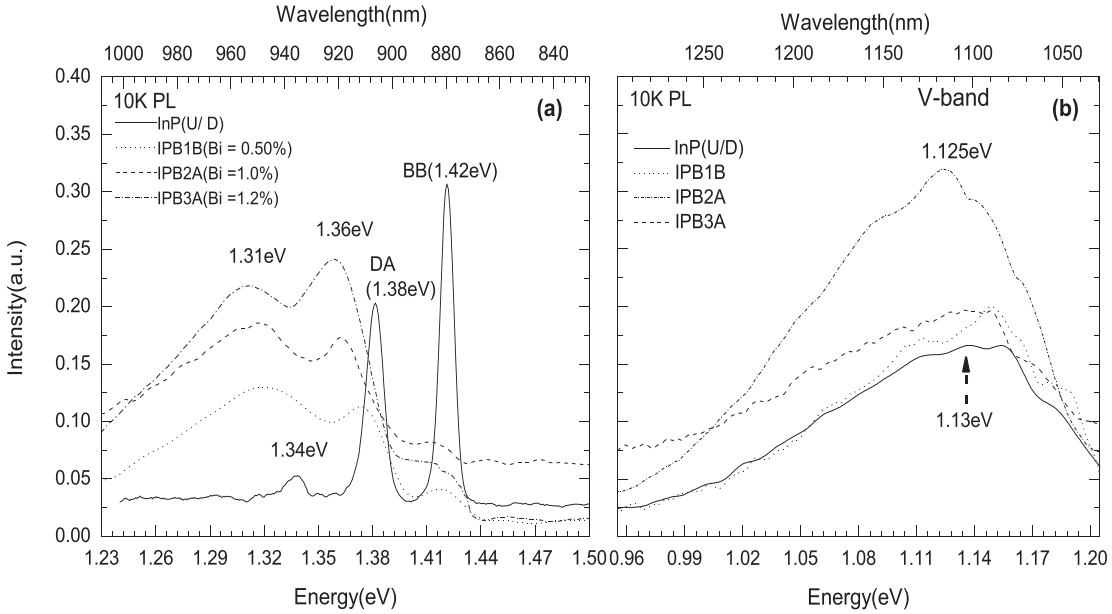

FIG. 5. 10 K photoluminescence spectra from InPBi layers contained with 0.5%, 1.0%, and 1.2% of Bi compared with undoped InP layer (solid line). (a) Lower energy side band and (b) the higher energy band.

corresponding lattice constants for indium containing III-V binaries shown in the inset of Fig. 6 and the VBO for InBi is found out to be 0.35 eV corresponding to its lattice constant of 6.686 Å and InBi spin orbit splitting (SO) energy of 2.2 eV estimated by the author of Ref. 26. Therefore, the values of VBO, conduction band offset (CBO), and spin-orbit split-off band offset between the endpoint compounds are found out to be 1.30 eV, −1.74 eV, and −0.69 eV, respectively. Now the position of the Bi related impurity level denoted by E_{Bi} is located 0.1 eV below the valence band maximum of InP and the atomic SO energy for Bi is 1.5 eV.[8] Thus, the location of corresponding spin-orbit split-off level $E_{Bi\text{-}SO}$ is 1.6 eV below the valence band maximum of InP

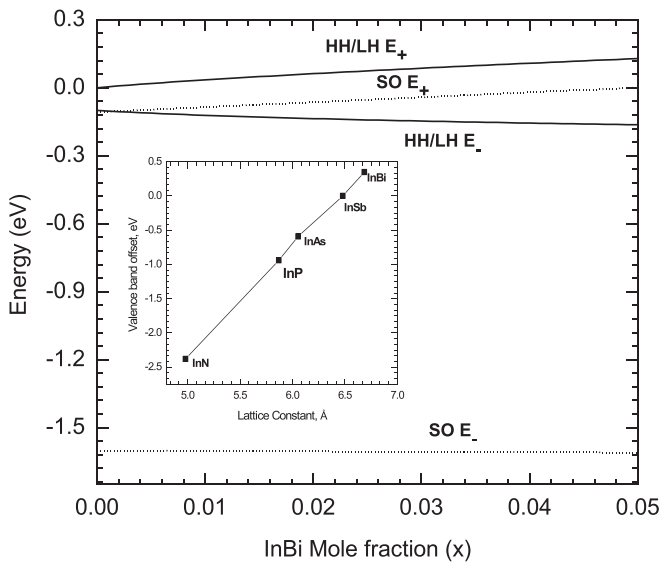

FIG. 6. Energy position of the E_+ and E_- related heavy, light, and spin-orbit split-off bands determined by the VBAC model as a function of InBi mole fraction. Plot of valence band offset versus lattice constant for In containing III-V binaries is shown in the inset figure (Ref. 31).

which is obtained from the value of the atomic SO energy for Bi. The theoretical band gap is defined as the difference in energy between the VBAC valence-band maximum and the virtual crystal approximation (VCA) conduction-band minimum (CBM) $E_{CB\text{-}VCA}$ which can be written as[8]

$$E_{CB-VCA} = E_g - \Delta E_{CBM},$$

where E_g is the band gap of InP and $\Delta E_{CBM} = 1.74$ eV is the edge of CBO between InP and InBi. The total band gap reduction is 52.1 meV/% Bi and according to this model the CBM moves downward by 17.4 meV/% Bi as predicted by VCA and the VBM moves upward by 34.7 meV/% Bi due to the VBAC interaction. We have found that there is a band gap reduction of about 66.5 meV for an incorporation of 1.2 at. % of Bi in InP. The calculated energy gap along with experimental PL result is displayed in Fig. 7. Using these values, we have found out the value of the fitting parameter, C_{Bi}, of 0.54 eV. The corresponding-band edge energy positions as a function of Bi concentration are shown in Fig. 6. Again the band gap bowing observed in $InP_{1-x}Bi_x$ is due to an upward movement of the heavy- and light-hole E_+ bands.

The PL spectra of all samples below 1.2 eV are shown in Fig. 5(b). All the samples showed a broad line centred at around 1.13 eV with shoulder at the higher and lower energy side and probably the reason for a marked asymmetry of the line shape, designated as the V band.[20] The V band is shifted by 10 meV due to incorporation of Bi and can be attributed to the free carrier-to-carrier bound to impurity or defect (FB) transition.

As shown in Fig. 8, when the excitation power density is increased, the emission shifts to high energy peaks measured at 10 K. This is because as the excitation power is increased the emission from the closest pairs saturates and recombination from the farthest pairs dominates.[27] With increasing the excitation power density from 0.18 to 0.56 W/cm^2, which did

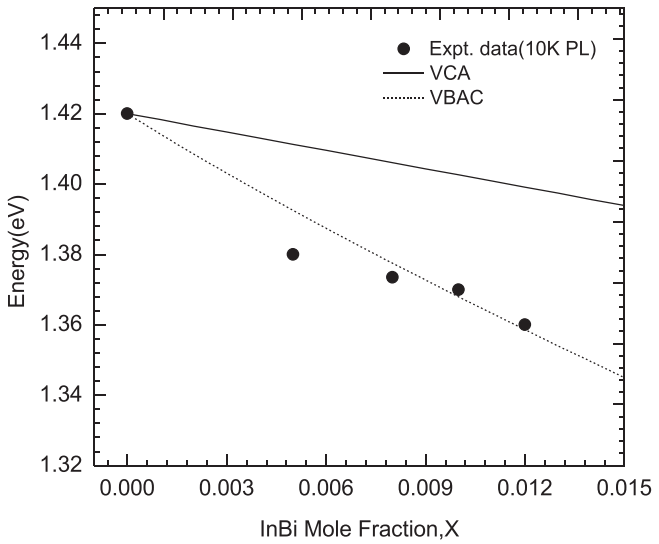

FIG. 7. Theoretically calculated bandgap of InPBi as a function of InBi mole fraction and compared with the experimental 10 K PL data as function of Bi composition (solid squares).

not show any peak at 1.42 eV where as when the power is increased from 0.82 to 1 W/cm^2 that can show the prominent peak at 1.42 eV due to BB transition from substrate.

The carrier density and electron mobility data were obtained the Van der Pauw technique on as-grown samples. Fig. 9 shows the mobility of $InP_{1-x}Bi_x$ for values of x ranging from 0% to 1.2% and obtain room temperature electron mobility in the range of 1950–2400 cm^2/V s, which confirm that the presence of Bi do not cause significant degradation of the electron mobility as was observed for other III-V-bismides.[28,29] The isolated Bi will form a resonant state in the valence band of InP because the 6p state of Bi is substantially higher than the 3p state of P, and Bi is likely to generate a potential trap for the holes and its effect the hole mobility rather than the electron mobility.[30] Scatter in the

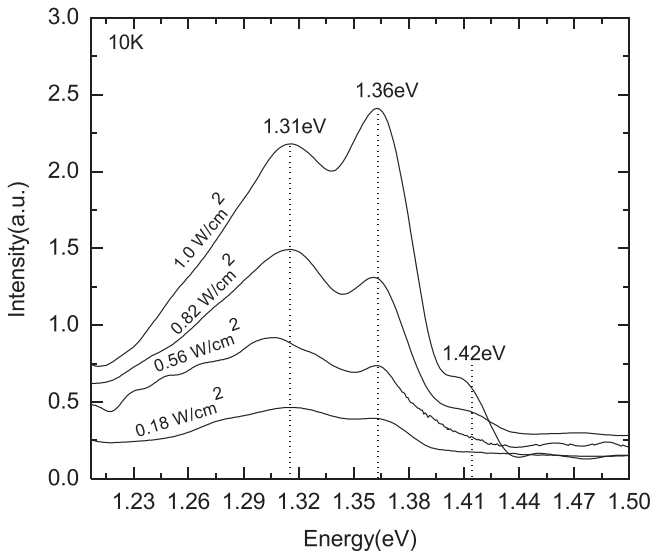

FIG. 8. PL curves for the sample with Bi = 1.2% at 10 K for different excitation powers.

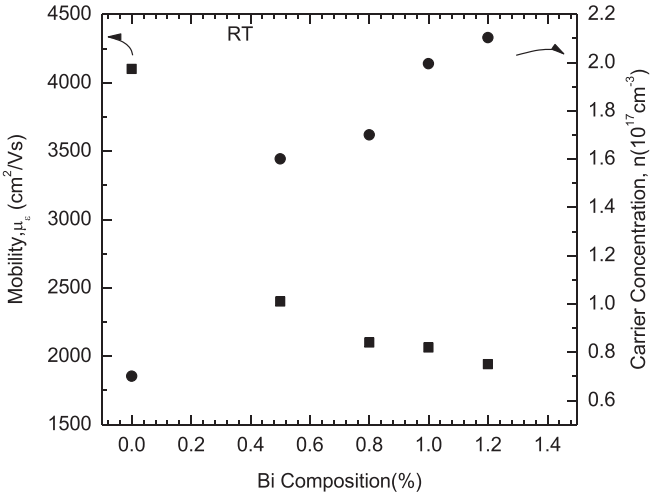

FIG. 9. Room temperature electron mobility (solid square) and carrier concentration (solid circle) of $InP_{1-x}Bi_x$ for different Bi concentrations.

data may be explained by the varying growth conditions such as growth temperature, as well as the unintentionally introduced impurity effects. The bulk carrier concentration ranged from 0.7×10^{17} to 2.104×10^{17} cm^{-3} and increases with the increase of Bi concentration.

IV. CONCLUSIONS

In summary, $InP_{1-x}Bi_x$ epilayers with Bi content up to x = 1.2% were grown on InP substrates by liquid phase epitaxy. The Bi incorporation was confirmed by SIMS. Clearly, resolved X-ray diffraction peaks suggested good crystalline quality of epitaxial layers and a lattice contraction was observed in the same experiment. Increased Bi content in the solid is found to reduce surface roughness down to about 42 nm. The 10 K PL spectrum shows that the band gap of InPBi for Bi content of 1.2% is reduced to 1.36 eV compared to the value of 1.42 eV for InP which amounts to a band gap reduction of approximately 50 meV/% Bi. The VBAC model indicates reduction of bandgap by about 52.1 meV/Bi% which agrees well with our experimental results. All samples exhibited negligible degradation in the electron mobility and moderate carrier concentration at room temperature.

ACKNOWLEDGMENTS

The author would like to acknowledge Professor S. Dhar, University of Calcutta for encouragement and many useful discussions. I gratefully acknowledge Mr. D. P. Samajdar for theoretical discussions. I thank Dr. Mukul Gupta, UGC-CSR, Indore for SIMS analysis of the samples. This work was supported by Department of Science and Technology, Government of India under Fast Track Project (SR/FTP/PS-89/2010).

[1]S. Francoeur, M.-J. Seong, A. Mascarenhas, S. Tixier, M. Adamcyk, and T. Tiedje, Appl. Phys. Lett. **82**, 3874 (2003).
[2]S. Tixier, M. Adamcyk, T. Tiedje, S. Francoeur, A. Mascarenhas, P. Wei, and F. Schiettekatte, Appl. Phys. Lett. **82**, 2245 (2003).

[3]K. Alberi, O. D. Dubon, W. Walukiewicz, K. M. Yu, K. Bertulis, and A. Krotkus, Appl. Phys. Lett. **91**, 051909 (2007).
[4]R. Kudrawiec, J. Kopaczek, P. Sitarek, J. Misiewicz, M. Henini, and S. V. Novikov, J. Appl. Phys. **111**, 066103 (2012).
[5]B. Fluegel, S. Francoeur, A. Mascarenhas, S. Tixier, E. C. Young, and T. Tiedje, Phys. Rev. Lett. **97**, 067205 (2006).
[6]F. A. Trumbore, M. Gershenzon, and D. G. Thomas, Appl. Phys. Lett. **9**, 4 (1966).
[7]P. J. Dean, A. M. White, E. W. Williams, and M. G. Astles, Solid State Commun. **9**, 1555 (1971).
[8]K. Alberi, J. Wu, W. Walukiewicz, K. M. Yu, O. D. Dubon, S. P. Watkins, C. X. Wang, X. Liu, Y.-J. Cho, and J. Furdyna, Phys. Rev. B **75**, 045203 (2007).
[9]S. K. Das, T. D. Das, S. Dhar, M. de la Mare, and A. Krier, Infrared Phys. Technol. **55**, 156 (2012).
[10]S. C. Das, T. D. Das, and S. Dhar, Infrared Phys. Technol. **55**, 306 (2012).
[11]D. P. Samajdar and S. Dhar, Semicond. Sci. Technol. **28**, 065007 (2013).
[12]A. V. Karimov, D. M. Yodgorova, and O. A. Abdulkhaev, J. Eng. Phys. Thermophys. **84**, 860 (2011).
[13]Y. Takehara, M. Yoshimoto, W. Huang, J. Saraie, K. Oe, A. Chayahara, and Y. Horino, Jpn. J. Appl. Phys., Part 1 **45**, 67 (2006).
[14]M. Masnadi-Shirazia, D. A. Beaton, R. B. Lewis, X. Lu, and T. Tiedje, J. Cryst. Growth **338**, 80 (2012).
[15]I. Moussa, H. Fitouri, A. Rebey, and B. El Jani, Thin Solid Films **516**, 8372 (2008).
[16]K. Y. Ma, Z. M. Fang, R. M. Cohen, and G. B. Stringfellow, J. Appl. Phys. **68**, 4586 (1990).
[17]Y. Song, S. Wang, I. Saha Roy, P. Shi, and A. Hallen, J. Vac. Sci. Technol., B **30**, 02B114 (2012).
[18]S. Tixier, M. Adamcyk, E. C. Young, J. H. Schmid, and T. Tiedje, J. Cryst. Growth **251**, 449 (2003).
[19]P. A. Postigo, F. Suárez, A. Sanz-Hervás, J. Sangrador, and C. G. Fonstad, J. Appl. Phys. **103**, 013508 (2008).
[20]P. W. Yu, B. W. Liang, and C. W. Tu, Appl. Phys. Lett. **61**, 2443 (1992).
[21]A. A. Iliadis and S. Ovadia, J. Appl. Phys. **63**, 5460 (1988).
[22]B. Wakefield, L. Eaves, K. A. Prior, A. W. Nelson, and G. J. Davies, J. Phys. D: Appl. Phys. **17**, L133 (1984).
[23]M. K. Rajpalke, W. M. Linhart, M. Birkett, K. M. Yu, D. O. Scanlon, J. Buckeridge, T. S. Jones, M. J. Ashwin, and T. D. Veal, Appl. Phys. Lett. **103**, 142106 (2013).
[24]J. Kopaczek, R. Kudrawiec, W. M. Linhart, M. K. Rajpalke, K. M. Yu, T. S. Jones, M. J. Ashwin, J. Misiewicz, and T. D. Veal, Appl. Phys. Lett. **103**, 261907 (2013).
[25]S. A. Barnett, J. Vac. Sci. Technol., A **5**, 2845 (1987).
[26]P. Carrier and S.-H. Wei, Phys. Rev. B **70**, 035212 (2004).
[27]R. N. Kini, A. J. Ptak, B. Fluegel, R. France, R. C. Reedy, and A. Mascarenhas, Phys. Rev. B **83**, 075307 (2011).
[28]D. G. Cooke, F. A. Hegmann, E. C. Young, and T. Tiedje, Appl. Phys. Lett. **89**, 122103 (2006).
[29]H. Oheda, Phys. Rev. B **71**, 155202 (2005).
[30]R. N. Kini, L. Bhusal, A. J. Ptak, R. France, and A. Mascarenhas, J. Appl. Phys. **106**, 043705 (2009).
[31]I. Vurgaftman, J. R. Meyer, and L. R. Ram-Mohan, J. Appl. Phys. **89**, 5815 (2001).